

A comparative analysis of torque ripple reduction techniques for sensor BLDC drive

Karthika Mahalingam¹, Nisha Kandencheri Chellaiah Ramji²

¹Department of Electrical and Electronics Engineering, New Horizon College of Engineering, Bangalore, India

²Department of Electronics and Communication Engineering, New Horizon College of Engineering, Bangalore, India

Article Info

Article history:

Received Jul 16, 2021

Revised Jan 23, 2022

Accepted Jan 30, 2022

Keywords:

BLDC

Charged capacitor

Comparative analysis

Cuk converter

DC-link voltage modulator

(DVM)

Torque ripple

ABSTRACT

Brushless direct current motors (BLDC) are prominent due to their high efficiency and less maintenance. However, BLDC motor applications are limited due to the requirement of a complex controller, the existence of torque ripple, and high cost. This research work describes the comparative analysis of different control strategies of torque ripple reduction in BLDC motors and it discusses various topologies viz. cuk converter, simple voltage modulator scheme, charged capacitor, Z-source inverter, and Quasi- Z source inverter-based torque ripple reduction techniques. The effectiveness of different control strategies has been verified using MATLAB Simulink and it helps to understand different control strategies for torque ripple reduction during the entire speed range. The analysis of MATLAB results reveal that the voltage modulation scheme reduces the torque ripple considerably during the entire speed range along with the noise-less operation of the BLDC motor when compared with other topologies.

This is an open access article under the [CC BY-SA](https://creativecommons.org/licenses/by-sa/4.0/) license.



Corresponding Author:

Karthika Mahalingam

Department of Electrical and Electronics Engineering, New Horizon College of Engineering

Bangalore, India

Email: karthikaganesh16@gmail.com

1. INTRODUCTION

Direct current (DC) motors used in speed and position control applications are prone to wear and tear, and maintenance issues due to the presence of brushes. These issues are overcome with BLDC motors [1]. BLDC motors are becoming popular in industrial applications owing to their high efficiency, less maintenance, high speed, long life, less electromagnetic interference, and less noise operation [2]. These motors are employed in medical, power-driven and hybrid vehicles, industrial robots, defense, and aerospace industries. The brushless motor has hall sensors to provide electronic commutation. The dissimilarity in the phase current leads to torque ripples during commutation in the trapezoidal back emf motors [3].

The torque fluctuation in BLDC motors is generated due to cogging torque and imperfections of back emf [4]. This torque ripple causes vibrations and acoustic noises which leads to undesirable stresses in bearings, mountings of the drive systems [5]. The discontinuity in torque is imprudent for the constant torque applications and it affects the reliability of the drive system. The effect of ripple is negligible in the low-speed range as compared to the high-speed operations [4]. The cause for the production of torque ripple, the speed versus torque characteristics and the impact of commutation time on non-commutated phase current have been discussed in detail [4]. The two different current control commutation topologies viz., DC-link sensing and DC current sensing have been analysed. The result shows that the ripple can be reduced by the influence of inductance in the machine design.

The expression for torque, the torque during conduction and the condition for minimum torque ripple have been analyzed in [5]. The relationship between speed and commutation time has been obtained for various values of speed [6]. The various control strategies for the torque ripple reduction have been listed in [7]. This includes comparison of different current and voltage control strategies of BLDC drive, features, emphasis, and applications of different control techniques. The torque ripple analysis and loss minimization techniques have been elucidated in detail [7]. A modified pulse width modulation (PWM) technique has been suggested to diminish the ripple owing to the mismatch between the energized and de-energized phase currents [8]. The PWM pulse duration is proportionate to the ratio of pulse duration to the commutation period. However, it has been observed that torque ripple reduction using PWM techniques can be used effectively for low- speed applications only [9].

A novel single ended primary inductor converter (SEPIC) with three-level neutral point converter (NPC) has been suggested to decrease the torque ripple during entire speed range [10]. The three-level converter reduces the torque ripple better than the two- level converter due to the application of half the supply voltage and reduces the harmonics which improves the efficiency. A Quasi-Z- source network has been proposed to diminish the torque ripple during the high-speed region [9]. The voltage is boosted using the Quasi-Z-source during the commutation period. A Z-source inverter (ZSI) has been suggested to diminish the ripple and to sense the end point of commutation[11]. A commutation time has been calculated using a comparator circuit with PWM without the calculation of commutation time [12].

A cuk converter control strategy [13] has been recommended during commutation to increase the supply voltage. The buck- boost mode regulates the input voltage using pulse amplitude modulation (PAM). A charged capacitor with two-phase modulation scheme has been stated [14] for the normal conduction and commutation periods. This avoids the need for mode selection circuit since the similar modulation technique has been used during the normal and commutation periods. A DC- link voltage modulator scheme has been reported to decrease the torque ripple [15]. This technique facilitates the commutating turn ON and turn OFF period and improves the DC- link supply during high speed. The ripple has been found to be diminished by a novel Integral variable structure control (IVSC) in which two- phase modulation is used [16]. A buck-boost converter has been used to regulate the phase current during commutation to minimize the ripple [17].

A single -input- dual- output (SIDO) converter is investigated [18] in which two voltage sources are used to supply the inverter and to increase the voltage during commutation. A novel topology using two- phase and three-phase conduction modes are mentioned to decrease the ripple throughout the regular and commutation period respectively [19]. A fuzzy logic based PI controller is proposed for the comparative analysis of BLDC motor [20]. A simple boost converter is mentioned in [21] to minimize the torque ripple with less storage elements.

The different optimization algorithms, analyses and applications have been discussed in [22]. A spider-based control algorithm has been suggested to minimize the ripple using a DC- link capacitor [23]. This algorithm restricts the use of large capacitor and switches and requires a simple and cost-effective BLDC drive. A. Alice Hepzibah et.al suggested an adaptive network-based fuzzy inference system (ANFIS) algorithm for a solar fed water pump system [24]. In this paper, various control approaches for the torque ripple reduction techniques are discussed. The variation on different parameters for the low- speed and high- speed ranges were analyzed. The simulation results provide adequate understanding of different control strategies of torque ripple reduction during the entire speed range.

2. MATHEMATICAL MODELLING OF BLDC MOTOR

The mathematical modelling of electrical machines gives the relation between its electromagnetic torque and other electrical and mechanical quantities. It is mainly used to obtain the performance parameters of a machine. The equivalent circuit of the BLDC drive system is shown in Figure 1.

It is assumed that the phase resistances $R_a = R_b = R_c$ and the self -inductances (L) and mutual inductances (M) are constant. The expression for phase voltages is given by (1).

$$\begin{bmatrix} V_{ab} \\ V_{bc} \\ V_{ca} \end{bmatrix} = \begin{bmatrix} R_a & 0 & 0 \\ 0 & R_a & 0 \\ 0 & 0 & R_a \end{bmatrix} \begin{bmatrix} i_a \\ i_b \\ i_c \end{bmatrix} + \frac{d}{dt} \begin{bmatrix} L & M & M \\ M & L & M \\ M & M & L \end{bmatrix} \begin{bmatrix} i_a \\ i_b \\ i_c \end{bmatrix} + \begin{bmatrix} e_a \\ e_b \\ e_c \end{bmatrix} \quad (1)$$

Where,

V_{ab}, V_{bc}, V_{ca} = Phase voltages (V)

i_a, i_b, i_c = Phase current (A)

e_a, e_b, e_c = Phase back emf (V)

We know that,

$$i_a + i_b + i_c = 0$$

$$\begin{bmatrix} V_{ab} \\ V_{bc} \\ V_{ca} \end{bmatrix} = \begin{bmatrix} R_a & 0 & 0 \\ 0 & R_a & 0 \\ 0 & 0 & R_a \end{bmatrix} \begin{bmatrix} i_a \\ i_b \\ i_c \end{bmatrix} + \frac{d}{dt} \begin{bmatrix} L - M & 0 & 0 \\ 0 & L - M & 0 \\ 0 & 0 & L - M \end{bmatrix} \begin{bmatrix} i_a \\ i_b \\ i_c \end{bmatrix} + \begin{bmatrix} e_a \\ e_b \\ e_c \end{bmatrix} \quad (2)$$

The stator voltage equation is given by,

$$V_{ab} = R_s i_a + (L - M) \frac{di_a}{dt} + e_a \quad (3)$$

$$V_{bc} = R_s i_b + (L - M) \frac{di_b}{dt} + e_b \quad (4)$$

$$V_{ca} = R_s i_c + (L - M) \frac{di_c}{dt} + e_c \quad (5)$$

Figure 2 shows the trapezoidal back emf, phase currents and gate pulses for the equivalent circuit of the BLDC motor. Table 1 gives the various parameters of the converter control circuit used in this paper.

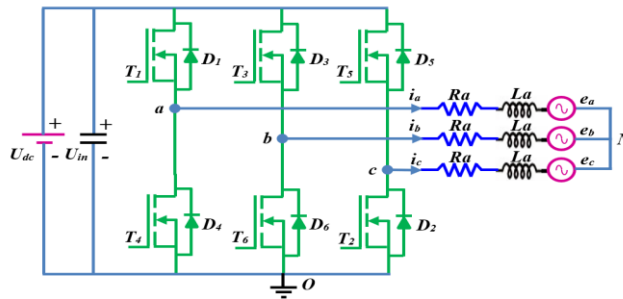


Figure 1. Equivalent circuit of the BLDC motor

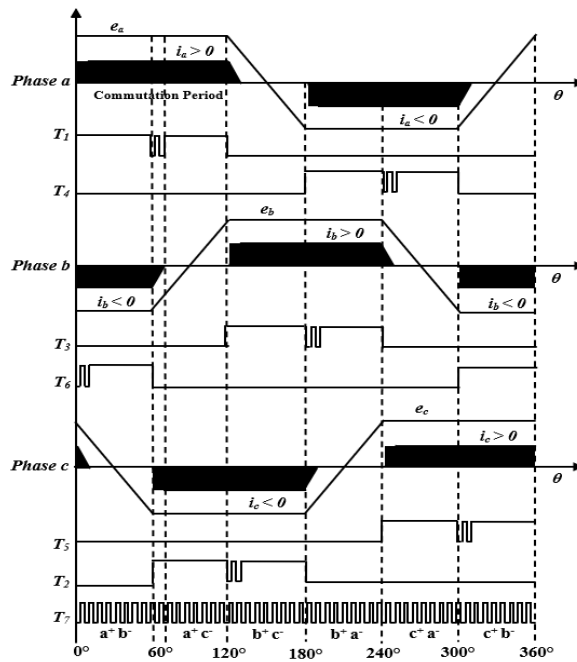


Figure 2. Trapezoidal back emf, phase currents and gate pulses of the BLDC motor

Table1. BLDC motor and different types of converter parameters

Motor type and different Converter topologies	Parameters	Values
Permanent magnet brushless DC (PMBLDC) motor	Voltage, V	24 V
	Power, P	70 W
	Rated current, I	4 A
	Rated load Torque, T	2 N/m
	Rated speed, N	3000 r/min
	Back EMF coefficient, k_e	0.028 V/(rad/s)
	Pairs of poles, p	5
	Resistance, R_{ph}	0.33 Ω
	Inductance, L	0.61 mH
	Cuk converter	Capacitance C_1
Capacitance C_2		2200 μ F
Inductance L_1		330 μ H
Inductance L_2		330 μ H
Charged capacitor converter	Capacitor	120 μ F
	Resistor	100 Ω
DC- link Voltage modulator	Capacitor C_1	4700 μ F
	Capacitor C_2	4700 μ F
	Inductor L	10 mH
ZSI	Inductance $L_1 = L_2$	330 μ H
	Capacitance $C_1 = C_2$	2200 μ F
	PWM carrier frequency	20 kHz
Quasi- ZSI	Inductance $L_1 = L_2$	200 μ H
	Capacitance $C_1 = C_2 = C_3$	470 μ F

3. ANALYSIS OF TORQUE RIPPLE IN A BLDC DRIVE

The torque equation is given by (6).

$$T_d = \frac{e_a i_a + e_b i_b + e_c i_c}{\omega} \quad (6)$$

Where,

T_d = developed electromagnetic torque (Nm)

ω = Rotor angular velocity (rad/sec)

The BLDC motor has three phases in which two phases are supplied with positive and negative energies and third phase is floating. The BLDC motor operated with six step commutations. Let, phase 'a' is positively energised, phase 'b' is negatively energised and phase 'c' is de-energised.

$$\begin{aligned} i_a &= -i_c; i_b = 0 \\ i_a &= -i_c = I \end{aligned} \quad (7)$$

Before commutation, the expression for the developed torque is (8).

$$T_d = \frac{E i_a + 0 - E(-i_a)}{\omega} = \frac{2E i_a}{\omega} = \frac{-2E i_c}{\omega} \quad (8)$$

After Commutation, the torque expression is given by (9).

$$T_d = \frac{2E i_b}{\omega} = \frac{-2E i_c}{\omega} \quad (9)$$

$i_b = -i_c = I = \text{Constant}$

During Commutation, the voltage equations and the torque expression are as follows;

$$R_a i_a + L_a \frac{di_a}{dt} + E + V_n = 0 \quad (10)$$

$$R_a i_b + L_a \frac{di_b}{dt} + E + V_n = V_{dc} \quad (11)$$

$$R_a i_c + L_a \frac{di_c}{dt} - E + V_n = 0 \quad (12)$$

$$T_d = \frac{2E(i_a + i_b)}{\omega} = \frac{-2E i_c}{\omega} \quad (13)$$

Hence the current i_c will remain constant for the condition of (14).

$$\frac{di_a}{dt} = -\frac{di_b}{dt} \quad (14)$$

The condition for minimum torque ripple can be obtained by adding the (10), (11) and (12) and simplifying,

$$V_{dc} = 4E \quad (15)$$

The (15) gives the minimum torque ripple condition [25]. The duty cycle (δ) expression during the conduction period is given by (16).

$$\begin{aligned} V_{dc_{nom}} \delta_{nom} &= -2R_a i_c + 2E \\ \delta_{nom} &= \frac{-2R_a i_c + 2E}{V_{dc_{nom}}} \end{aligned} \quad (16)$$

4. ANALYSIS OF DIFFERENT TORQUE RIPPLE REDUCTION TOPOLOGIES

In this paper, various control approaches for the torque ripple reduction techniques have been explored. The effect of varying different parameters on torque ripple for the entire speed range has been analyzed. This paper discusses various topologies such as cuk converter, simple voltage modulator scheme, charged capacitor, Z-Source inverter, and Quasi- Z source inverter-based torque ripple reduction techniques.

4.1. Cuk converter topology

The cuk converter in Figure 3 is suggested [13] to improve the input voltage during the commutation interval. The switch T_s and diode D_s are used as the mode selection circuit. The normal conduction is enabled when the switch T_s is off and diode D_s is forward biased to drive the BLDC drive through the DC supply voltage. During this mode of operation, the inverter input voltage can be controlled by the speed and current control strategy without the PWM scheme. The switch T_s is closed and diode D_s is open during commutation and the converter is operating in boost mode. In this condition, the DC input voltage can be increased by adding the capacitor voltage.

The proposed strategy performance is verified under rated conditions shown in Table 1 of a BLDC motor drive with a speed of 1500 rpm and torque of 2 Nm. This topology has many advantages such as reduction in torque ripple, PAM technique evades the voltage spikes during turn on and off switches and simple modulation scheme.

4.2. Charged Capacitor Control Strategy

Figure 4 shows the charged capacitor topology [14]. The capacitor C charges through the diode by keeping switch S_1 off and S_2 on during normal interval. This charged voltage is added with the supply voltage during commutation period by turning on S_1 and turning off S_2 . In this method the input voltage is boosted using charged capacitor during commutation period. This topology does not require DC-DC converter, uses two-phase modulation during both the conduction periods and the voltage stress can be reduced without the use of inductors.

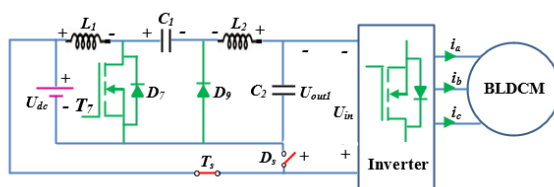


Figure 3. Cuk converter during commutation

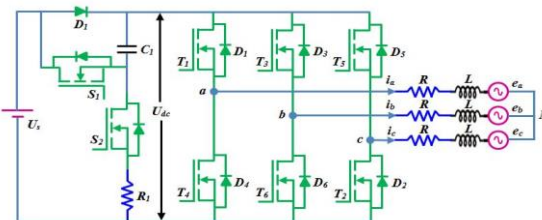


Figure 4. Charged capacitor control strategy

4.3. Z source inverter topology

The shoot through state of ZSI in Figure 5 is a forbidden state in voltage and current source inverters because of output voltage distortion and higher current rating which may damage the circuit. But in ZSI, this

shoot through state is possible and it improves the performance of power conversion. In this topology, a novel non-commutated phase current stabilization and commutation end point detection were proposed [11]. The zero-crossing point of back electromotive force (EMF) can be obtained by comparing all phase voltages with zero reference voltage. The ZSI improves the DC voltage utilization, enhances the safety and reliability of the system. This method avoids the need of additional current sensors for the commutation end point detection and does not require extra resistances and inductances.

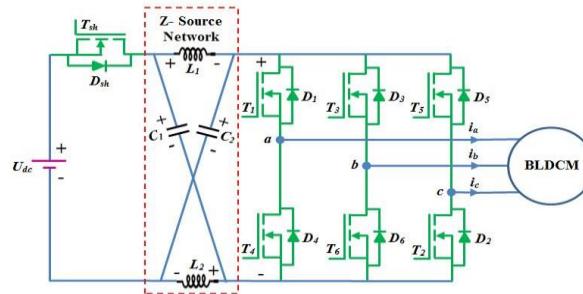


Figure 5. ZSI based BLDC drive system for torque ripple reduction

4.4. Quasi-Z source inverter topology

The torque ripple during the high-speed operation can be reduced using high gain and smooth reliability characteristics of the Quasi-Z- source inverter [9]. The PWM technique is employed to regulate the speed and the torque ripple. During the non- shoot-through state, the metal oxide semiconductor field effect transistor (MOSFET) is open and L_1 and L_2 supplies the energy to the load and capacitor C_1 stores the energy. During shoot-through state, the MOSFET is closed and the capacitor C_2 supplies the load. The boosted voltage can be obtained from the inductor currents L_1 and L_2 . The switch over from DC supply to Quasi-Z-source network can be accomplished using a power selection circuit and a switch as shown in Figure 6. This reduces the commutation interval delay of the Quasi-Z-source network. This topology is applicable for fans and servo motor systems, and it gives high reliability and improved efficiency.

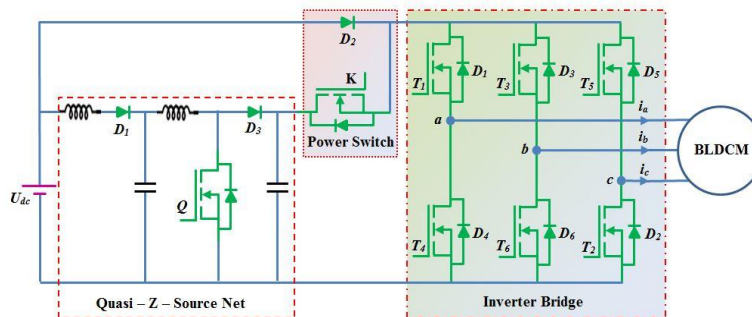


Figure 6. Quasi-Z-source inverter

4.5. DC- link voltage modulator scheme

The DC- link Voltage Modulator (DVM) scheme uses switches S_1 and S_2 , capacitors C_1 and C_2 , an inductor L and diode D for the reduction of torque ripple [15]. During normal conduction period S_1 is off and S_2 is on and both the capacitors are charged. During commutation period the switch S_1 is on and S_2 is off so that both the capacitors can be connected in series to boost the input voltage. This topology is functionally same as the cuk converter topology and the main difference exist in the modulation scheme. This is achieved by connecting two capacitors as shown in Figure 7. The DVM scheme reduces the torque ripple comparatively better than the cuk converter and charged capacitor method. This method reduces the torque ripple during entire speed range, simple additional components are required to boost the input voltage and better reduction in torque ripple which leads to noise-free and smooth operation of BLDC motor.

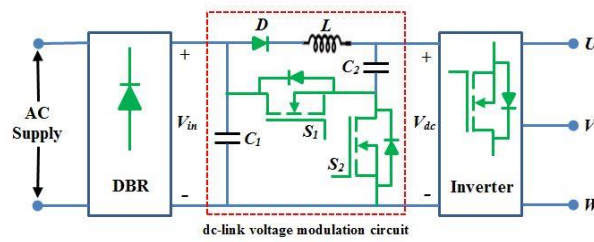


Figure 7. DC link voltage modulator scheme

5. RESULTS AND DISCUSSIONS

This paper compares the various control topologies for the torque ripple reduction. The analysis of stator current and torque ripple is discussed in detail. The torque, speed and stator current of the conventional and cuk converter-based torque ripple reduction techniques are shown in Figures 8 (a) and 8 (b). Figure 9 (a) shows the zoom view of torque waveforms for 500 rpm of 5 Nm load torque whereas and Figure 9 (b) illustrates the torque waveform with 1500 rpm using cuk converter respectively. The 7.2% of non-commutated phase current fluctuation is reduced than the traditional strategy. The high-frequency interference issues of MOSFET switch can be reduced by varying the inverter input voltage by PAM scheme during the normal conduction period.

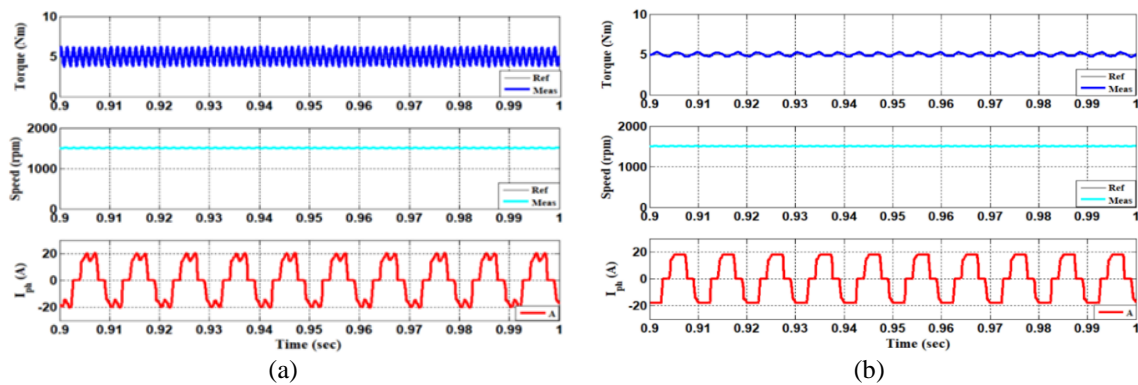


Figure 8. Torque, speed and stator current with (a) constant load torque of 5 Nm with 1500 rpm of the Conventional method and (b) constant load torque of 5 Nm with 1500 rpm of the cuk converter method

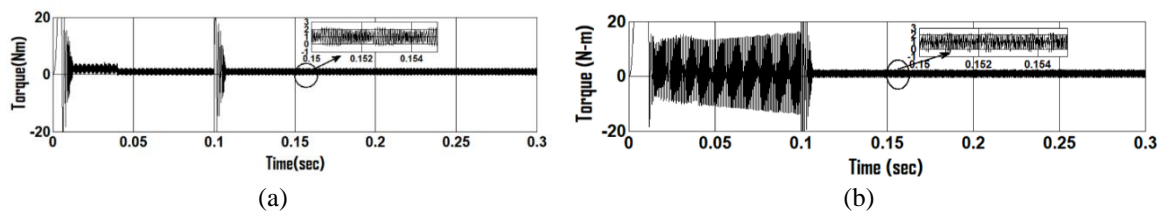


Figure 9. cuk converter method (a) zoom view of torque waveforms for 500 rpm of 2 Nm load torque and (b) zoom view of torque waveforms for 1500 rpm

The torque ripple using charged capacitor method is shown in Figures 10 (a) and (b) for the 500 rpm and 1500 rpm with 2 Nm load torque respectively. The ripple is reduced compared to the traditional method using the boosted DC- link voltage. The current and torque ripple are reduced 20% more than the conventional method. The ZSI topology reduces the current ripple considerably than the other torque ripple reduction techniques. The non- commutated current fluctuation as shown in Figures 11 (a) and 11(b) can be reduced by 8.4% which is 23% more than the conventional method in heavy load conditions. The ZSI improves the DC voltage utilization, enhances the safety and reliability of the system. This method avoids the need for additional

current sensors for the commutation end point detection and does not require extra resistances and inductances. The PWM modulation scheme is simplified compared to three-phase modulation techniques and reduces the number of MOSFET switches and its driver circuit.

The torque ripple waveforms are obtained for 2 Nm load torque with 500rpm speed using Q-ZSI is depicted in Figure 12 (a). The torque ripple for the high-speed range of 1500 rpm is revealed in Figure 12 (b). The torque ripple is reduced by 6.5% during high speed and 8.7% during low speed. The switch over from DC supply to Quasi-Z-source network can be accomplished using a power selection circuit and a switch. This reduces the commutation interval delay of the Quasi-Z-source network. This topology is applicable for fans and servo motor systems, and it gives high reliability and improved efficiency.

The torque waveforms using DVM converter during 500 rpm and 1500 rpm in Figures 13 (a) and 13 (b) shows that the torque ripple reduction is 6% which is better than other topologies. The analysis of MATLAB result shows that the voltage modulation scheme has a better torque ripple reduction than other topologies. This method diminishes the torque ripple during entire speed range with the noise less operation of BLDC motor. Table 2 shows the torque ripple analysis for the different topologies.

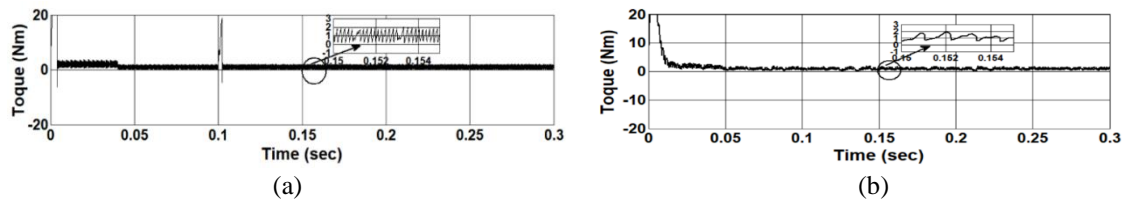


Figure 10. Charged capacitor method (a) zoom view of torque waveforms at 500 rpm and (b) zoom view of torque waveforms at 1500 rpm

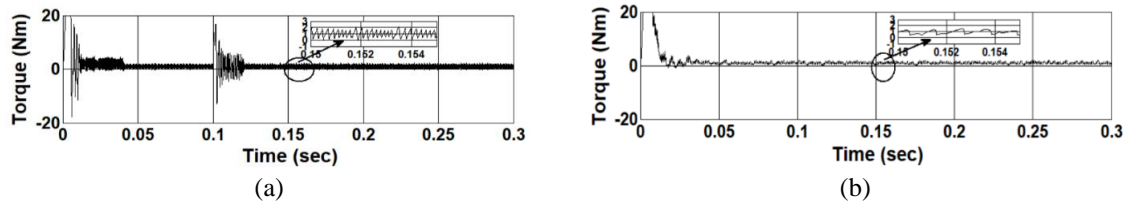


Figure 11. ZSI method (a) zoom view of torque waveforms at 500 rpm and (b) zoom view of torque waveforms at 1500 rpm using ZSI

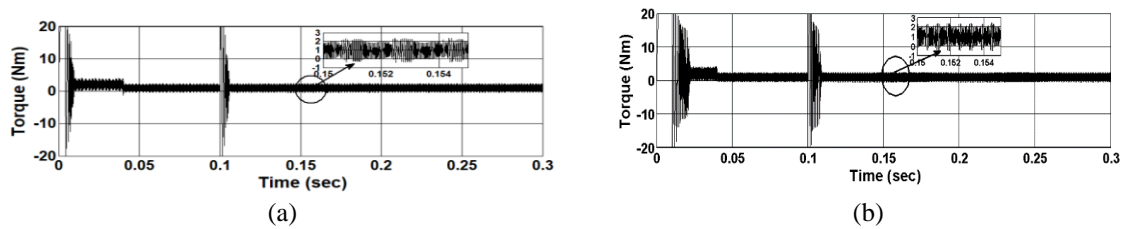


Figure 12. QZSI method (a) zoom view of torque waveforms at 500 rpm and (b) zoom view of torque waveforms at 1500 rpm

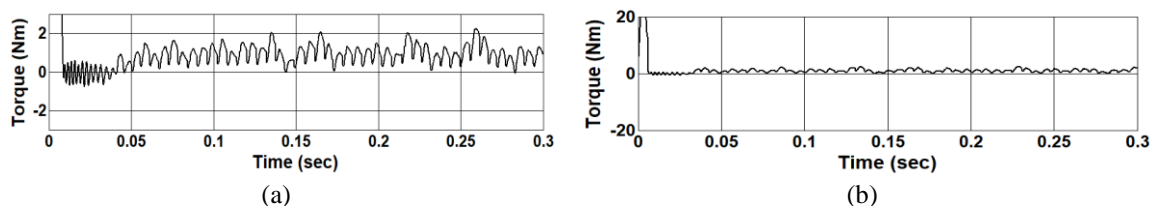


Figure 13. DVM method (a) zoom view of torque waveforms at 500 rpm and (b) zoom view of torque waveforms at 1500 rpm

Table 2. Torque ripple analysis

Topologies	Load Torque (Nm)	Torque ripple (%) at 1500 rpm	Torque ripple (%) at 500 rpm
Cuk converter	2	7.5%	11%
Charged capacitor converter	2	23.4%	20%
ZSI	2	18%	22%
Quasi- ZSI	2	27%	25%
DC- link Voltage modulator	2	5.5%	7.5%

6. CONCLUSION

This paper encompasses the comparative analysis of various control techniques for the torque ripple reduction topologies such as cuk converter, simple voltage modulator scheme, charged capacitor, Z-Source inverter, and Quasi-Z source inverter have been deliberated. Each strategy has its own advantages and disadvantages from different perspectives. The cuk converter topology has resulted in 7.5% of torque ripple minimization during high- speed region and 11% of torque ripple minimization in low- speed region whereas charged capacitor method has resulted in 20% of torque ripple reduction. The DVM method gives better performance than all other topologies by providing 5.5% of torque ripple reduction during high- speed region. The simulation results validates that the DVM has a better torque ripple reduction during entire speed range with the noise- less operation of BLDC motor with less components.




REFERENCES

- [1] S.-H. Kim, "Brushless direct current motors," *Electr. Mot. Control*, no. Dc, pp. 389–416, 2017, doi: 10.1016/b978-0-12-812138-2.00010-6.
- [2] B. Singh and S. Singh, "State of the art on permanent magnet brushless DC motor drives," *J. Power Electron.*, vol. 9, no. 1, pp. 1–17, 2009, doi: 10.6113/JPE.2009.9.1.1.
- [3] K. Y. Cheng and Y. Y. Tzou, "Design of a Sensorless Commutation IC for BLDC Motors," *IEEE Trans. Power Electron.*, vol. 18, no. 6, pp. 1365–1375, 2003, doi: 10.1109/TPEL.2003.818867.
- [4] R. Carlson, M. Lajoie-Mazenc and J. C. do S. Fagundes, "Analysis of Torque Ripple Due to Phase Commutation in Brushless dc Machines," *IEEE Trans. Ind. Appl.*, vol. 28, no. 3, pp. 632–638, 1992, doi: 10.1109/28.137450.
- [5] H. K. Samitha Ransara and U. K. Madawala, "A Torque Ripple Compensation Technique for a Low-Cost Brushless DC Motor Drive," *IEEE Trans. Ind. Electron.*, vol. 62, no. 10, pp. 6171–6182, 2015, doi: 10.1109/TIE.2015.2423664.
- [6] B. H. Kang, C. J. Kim, H. S. Mok, and G. H. Choe, "Analysis of torque ripple in BLDC motor with commutation time," *IEEE Int. Symp. Ind. Electron.*, vol. 2, no. 1, pp. 1044–1048, 2001, doi: 10.1109/isie.2001.931619.
- [7] S. A. K. Mozaffari Niapour, GH. Shokri Garjan, M. Shafiei, M. R. Feysi, S. Danyali, and M. Bahrami Kouhshahi, "Review of Permanent-Magnet brushless DC motor basic drives based on analysis and simulation study," *Int. Rev. Electr. Eng.*, vol. 9, no. 5, pp. 930–957, 2014, doi: 10.15866/iree.v9i5.827.
- [8] W. A. Salah, D. Ishak, and K. J. Hammadi, "PWM switching strategy for torque ripple minimization in BLDC motor," *J. Electr. Eng.*, vol. 62, no. 3, pp. 141–146, 2011, doi: 10.2478/v10187-011-0023-1.
- [9] K. Xia, J. Lu, C. Bi, Y. Tan, and B. Dong, "Dynamic commutation torque-ripple reduction for brushless DC motor based on quasi-Z-source net," *IET Electr. Power Appl.*, vol. 10, no. 9, pp. 819–826, 2016, doi: 10.1049/iet-epa.2016.0219.
- [10] V. Visvanathan and S. Jeevanathan, "Approach for torque ripple reduction for brushless DC motor based on three-level neutral-point-clamped inverter with DC-DC converter," *IET Power Electron.*, vol. 8, no. 1, pp. 47–55, 2015, doi: 10.1049/iet-pel.2013.0471.
- [11] X. Li, C. Xia, Y. Cao, W. Chen, and T. Shi, "Commutation Torque Ripple Reduction Strategy of Z-Source Inverter Fed Brushless DC Motor," *IEEE Trans. Power Electron.*, vol. 31, no. 11, pp. 7677–7690, 2016, doi: 10.1109/TPEL.2016.2550489.
- [12] Y. K. Lin and Y. S. Lai, "Pulsewidth modulation technique for BLDCM drives to reduce commutation torque ripple without calculation of commutation time," *IEEE Trans. Ind. Appl.*, vol. 47, no. 4, pp. 1786–1793, 2011, doi: 10.1109/TIA.2011.2155612.
- [13] W. Chen, Y. Liu, X. Li, T. Shi, and C. Xia, "A novel method of reducing commutation torque ripple for brushless DC motor based on Cuk converter," *IEEE Trans. Power Electron.*, vol. 32, no. 7, pp. 5497–5508, 2017, doi: 10.1109/TPEL.2016.2613126.
- [14] X. Yao, J. Zhao, J. Wang, G. Lu, and F. Wang, "A novel method of commutation torque ripple reduction for BLDC with charged capacitor," *Chinese Control Conf. CCC*, vol. 2018-July, pp. 3736–3740, 2018, doi: 10.23919/ChiCC.2018.8482609.
- [15] R. K. Achary, S. Durgaprasanth, C. Nagamani, and G. S. Ilango, "A Simple Voltage Modulator Scheme for Torque Ripple Minimization in a Permanent Magnet Brushless DC Motor," *IEEE Trans. Power Electron.*, vol. 35, no. 3, pp. 2809–2818, 2020, doi: 10.1109/TPEL.2019.2926122.
- [16] C. Xia, Y. Xiao, W. Chen, and T. Shi, "Torque ripple reduction in brushless DC drives based on reference current optimization using integral variable structure control," *IEEE Trans. Ind. Electron.*, vol. 61, no. 2, pp. 738–752, 2014, doi: 10.1109/TIE.2013.2254093.
- [17] K. Rajesh, S. Durgaprasanth, C. Nagamani, and G. Saravana Ilango, "A Buck-Boost Converter with DC Link Voltage Boost for Minimizing Torque Ripple in Brushless DC Motor," *2018 20th Natl. Power Syst. Conf. NPSC 2018*, pp. 1–6, 2018, doi: 10.1109/NPSC.2018.8771853.
- [18] B. N. Kommula and V. R. Kota, "A novel scheme for torque ripple minimization of BLDC motor used in solar air conditioner," *Electr. Eng.*, vol. 100, no. 4, pp. 2473–2483, 2018, doi: 10.1007/s00202-018-0721-9.
- [19] Z. Li, Q. Kong, S. Cheng, and J. Liu, "Torque ripple suppression of brushless DC motor drives using an alternating two-phase and three-phase conduction mode," *IET Power Electron.*, vol. 13, no. 8, pp. 1622–1629, 2020, doi: 10.1049/iet-pel.2019.0960.
- [20] A. H. Ahmed, A. E. S. B. Kotb, and A. M. Ali, "Comparison between Fuzzy Logic and PI Control for The Speed Of BLDC Motor," *Int. J. Power Electron. Drive Syst.*, vol. 9, no. 3, p. 1116, 2018, doi: 10.11591/ijpeds.v9.i3.pp1116-1123.
- [21] K. Vengadakrishnan, N. Madhanakkumar, P. Pugazhendiran, C. Bharatiraja, and V. Sriramkumar, "Torque ripple minimization of PMBLDC motor using simple boost inverter," *Int. J. Power Electron. Drive Syst.*, vol. 10, no. 4, p. 1714, 2019, doi: 10.11591/ijpeds.v10.i4.pp1714-1723.




- [22] A. Darwish, "Bio-inspired computing: Algorithms review, deep analysis, and the scope of applications," *Futur. Comput. Informatics J.*, vol. 3, no. 2, pp. 231–246, 2018, doi: 10.1016/j.fcij.2018.06.001.
- [23] M. P. Maharajan and S. A. E. Xavier, "Design of Speed Control and Reduction of Torque Ripple Factor in BLdc Motor Using Spider Based Controller," *IEEE Trans. Power Electron.*, vol. 34, no. 8, pp. 7826–7837, 2019, doi: 10.1109/TPEL.2018.2880916.
- [24] A. Alice Hepzibah and K. Premkumar, "ANFIS current–voltage controlled MPPT algorithm for solar powered brushless DC motor based water pump," *Electr. Eng.*, vol. 102, no. 1, pp. 421–435, 2020, doi: 10.1007/s00202-019-00885-8.
- [25] M. Karthika and K. C. R. Nisha, "Review on Torque Ripple Reduction Techniques of BLDC Motor," in *2020 International Conference on Inventive Computation Technologies (ICICT)*, Feb. 2020, pp. 1092–1096, doi: 10.1109/ICICT48043.2020.9112523.

BIOGRAPHIES OF AUTHORS



Karthika Mahalingam    received her B.E degree in Electrical and Electronics Engineering from M K university, Madurai in 2002. She received M.E in Power Electronics and drives from Anna university in 2012. She is working as a senior Assistant professor in Department of Electrical and Electronics Engineering, New Horizon College of Engineering, Bangalore. Currently, she is pursuing Ph.D in New Horizon College of Engineering, Bangalore, Visvesvaraya Technological University, Belagavi, Karnataka, India. Her research interest includes BLDC drives, Power Electronics controllers, and Renewable energy sources. She can be contacted at email: karthikaganesh16@gmail.com.



Nisha Kandancheri Chellaiah Ramji    received her B.E degree in Electronics and Communication Engineering from Bharathidasan University, Trichy in 2002. She received M.E in Power Electronics and Ph.D in Power Converters for Renewable Energy Systems from Sathyabama University, Chennai in 2004 and 2015 respectively. She started her career as lecturer in Sathyabama University (2003-2009). She joined New Horizon College of Engineering, Bangalore in 2009 and currently working as a Professor at the Department of Electronics and Communication Engineering. She has more than 16 years of academic cum research experience at university and college level. Her contributions are accorded in the field of efficient Power Converters for Renewable Energy systems and Embedded control of Power applications. She is currently Vice chair of IEEE Industrial Electronics Society - Bangalore chapter (IES 2021), Publication chair- Joint IEEE PEL/IES Bangalore chapter (2021), Point of Contact (PoC) for UNISEC India Local Chapter Bangalore Section, ISRO -IIRS Coordinator of NHCE Student branch counsellor of NHCE IEEE and MTS NHCE chapters. She can be contacted at email: nishashaji@gmail.com.